Effect of Laser Parameters on PMMA during Laser Micromachining: A FEMLAB Simulation

R. Ndeda, P. N. Kioni and J. N. Keraita

Abstract—Laser micromachining has been widely applied in the fabrication, production and manufacturing of Micro Electro Mechanical Systems (MEMS). It uses photo thermal melting or ablation to fabricate a microstructure. The use of heat as a means of material removal has various negative effects on different materials. Distortion of the material is one of the negative effects, especially polymers.

Polymers are often used in medical devices, microelectronic and sensor industries where high precision and high quality is required. During laser cutting of polymers, bulges are formed mainly due to resolidification of molten material in the working zone and temperature difference between the heat affected zone and the heat unaffected zone.

A mathematical model has been developed using finite element analysis to model polymer material behavior during laser cutting. The model was run on both FEMLAB and MATLAB softwares. The effects of cutting parameters on bulge formation was then be analyzed and the results compared to theoretical structures.

Keywords—FEMLAB, finite element, polymers, laser micromachining

I. Nomenclature

Bi	Biot number
c	specific heat (J/kg.K)
T	temperature (K)
F	absorbed laser beam flux (W/m^2)
X, Y, Z	spatial coordinates
X_F, Y_F, Z_F	half the x,y,z dimensions of the specimen
$\hat{i}$, $\hat{k}$	unit vectors in the X, Z directions respectively
I	intensity of radiation (W/m^2)
$\hat{n}$	unit outward surface normal
R_0	laser beam radius at focal point (m)
h_c	convection heat transfer coefficient (W/m^2.K)
k	thermal conductivity (W/m.K)
h_f	heat of fusion (J/kg)
h_g	heat of vaporization (J/kg)
u	scanning velocity in x-direction (mm/s)
v_n	ablation velocity in normal direction (mm/s)
T_s	temperature at the interface (K)
T_v	temperature at the vapor side (K)
T_∞	ambient temperature
$\hat{n}$	direction of the normal
t	time (s)
Δg_v	free energy of removal at ablation (J/kg)
ΔH_v	enthalpy of removal at ablation (J/kg)

Greek letters

α_0	absorptivity (μm^{-1})
α	thermal diffusivity (m^2/s)
∇	differential del operator.
ρ	polymer material density (kg/m^3)
λ_L	primary wavelength of the laser beam (μm)

R. Ndeda, Department of Mechatronic Engineering, Jomo Kenyatta University of Agriculture and Technology (phone: +2540735100441; fax: +2546752711; (e-mail: reheman@eng. jkuat.ac.ke).

P. N. Kioni, Department of Mechanical Engineering, Jomo Kenyatta University of Agriculture and Technology (e-mail: pnkioni@eng. jkuat.ac.ke).

J. N. Keraita, Department of Mechatronic Engineering, Jomo Kenyatta University of Agriculture and Technology (e-mail: keraitajn@eng. jkuat.ac.ke).

II. Introduction

LASER micromachining has developed greatly over the last two decades. It is a method which uses photothermal melting to fabricate a part. CO_2 lasers are often preferred in laser cutting of polymers. This is due to its suitable characteristics such as relatively long wavelength and diffraction limit.

During laser cutting of polymers, the material experiences various stresses, mostly, thermal stresses which occur due to the different thermal properties between the heat affected zone and the heat unaffected zone on the material. The sharp temperature gradient causes distortion. This distortion may be in the form of bulges or humps. These bulges around the machined area can cause abrasion or irritation especially on parts that move against another surface. They may also cause reduction of bonding quality of the region.

The effects of laser cutting on polymers is a subject of recent and current research. Formation of bulges during laser micromachining of polymers has been attributed to various causes. Chung [1] attributed formation of bulges to two mechanisms. One, called the conventional bulge, as shown in figure 1 is formed from the thermal molten polymer resolidified by atmospheric air cooling on the rim of the channel after splashing from high-pressure gas or surface tension driven flow. The other, called a hump, is formed due to the thermal distortion from thermal stress or residual stress in a large temperature gradient.

Snakenborg [2] attributed bulge formation to lowering of the polymer density as a result of the irradiation, resulting in an increase in volume and, therefore, a rising of the polymer material. He asserted that the density was presumably lowered in the heating-up process, where several polymer chains were already cut into shorter chains without being ablated.

This bulge is disadvantageous during micromachining. There is therefore need for detailed research to reduce the formation of this bulge without increasing machining time. Methods previously suggested include covering the polymer substrate with a photresist layer [1] and preheating the polymer material before cutting [**?**].

This paper focuses on the development of a three-dimensional finite element-based model is developed, using

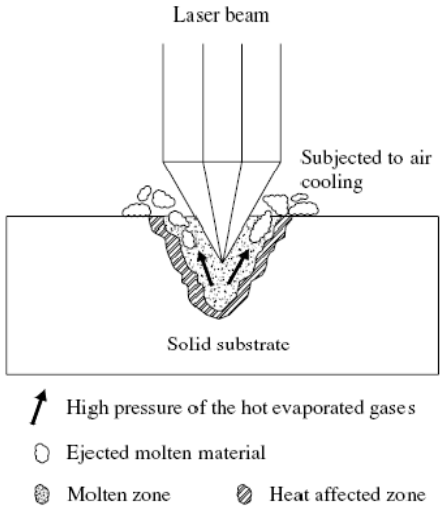

Fig. 1. The schematic model of the bulge formation of polymer micromachined by a laser beam through splashing and resolidification [1].

the commercial code FEMLAB and MATLAB.This is done in order to predict temperature distribution in the polymer Polymethylmethacrylate(PMMA) during CO_2 laser cutting.

The effect of laser cutting process parameters on PMMA are studied. These parameters are laser beam velocity and laser power. The effects of these parameters on the temperature distribution are then analyzed.

III. MATHEMATICAL DESCRIPTION

The mathematical description of the proposed model is reported as follows: A brick-type solid irradiated by a moving heat source is considered. The solid dimension along the motion direction is assumed to be semi-infinite, while finite thickness and width are assumed. A two-dimensional(2D) model is assumed. Radiative and convective heat losses are taken into account. The thermophysical properties of the material are assumed to be constant. The conductive model is also considered transient.

According to the moving heat source theory [4], a coordinate system fixed to the heat source is chosen. The mathematical statement of the problem is:

$$-\nabla.(q_c + \delta q_d) = \rho c_p \frac{\partial T}{\partial t} \tag{1}$$

where q_d is the radiative heat flux, q_c is the conductive heat flux, ρ is the density of the material, c_p is the heat capacity and T is the temperature. δ=1 due to the transparent material used. The heat equation therefore becomes

$$\nabla^2 T + \nabla.q_d = \frac{\rho c_p}{k}\frac{\partial T}{\partial t} \tag{2}$$

The initial condition for all the nodes of the workpiece is given by

$$T(x, y, 0) = 293.0K \tag{3}$$

A sketch of the configuration is shown in Fig 2.

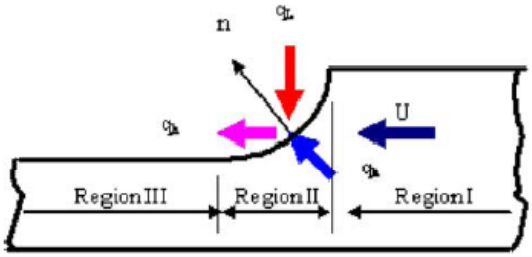

Fig. 2. Energy balance on the surface subject to laser [3]

The upper surface boundary condition is broken down into three regions; the first region is the laser unimpinged zone, the second region is the laser impinged zone and the last is the already machined zone. The boundary conditions are described as follows:

Region I-Laser unimpinged zone

$$\begin{aligned} &a\vec{F}\hat{n} = -\hat{n}(k\nabla T) + h_c(T - T_\infty) + \epsilon\sigma(T^4 - T_\infty^4) \\ &at\ y = S(x),\ x_{min} < x < x_{max} \\ &and\ T_s = T_v(1 + \frac{h_g}{C_p T_v} + \frac{RT_v}{h_g}) \end{aligned} \tag{4}$$

Region II-Impinged zone

$$\begin{aligned} &a\vec{F}\hat{n} = -\hat{n}(k\nabla T) + h_c(T - T_\infty) + \epsilon\sigma(T^4 - T_\infty^4) \\ &+ v_n\rho\Delta H_v \\ &at\ y = S(x),\ x_{min} < x < x_{max} \\ &and\ T_s = T_v(1 + \frac{h_g}{C_p T_v} + \frac{RT_v}{h_g}) \end{aligned} \tag{5}$$

Region III- machined zone

$$\begin{aligned} &\frac{\partial T}{\partial y} = 0 \\ &at\, y = S(x_c),\ x_{2F} - x_c < x < x_{2F} \end{aligned} \tag{6}$$

where h_c is the convection heat transfer coefficient, T_∞ is the ambient temperature, ϵ is the emissivity, σ is the Planck's constant, v_n is the velocity, ΔH_v is the enthalpy of vaporization, T_v is the temperature of vaporization, T_s is the temperature at the interface, h_g is the heat of vaporization and R is the beam radius.

The boundary at the bottom of the workpiece is given by:

$$\begin{aligned} &\frac{\partial T}{\partial y} = 0 \\ &at \quad y = y_F, -x_F < x < (x_{2F} - x_F) \end{aligned} \tag{7}$$

where the subscripts F and 2F denote the value of y at full dimension and the value of x at full dimension respectively. An adiabatic boundary condition is applied to the left and right side of the workpiece.

$$\begin{aligned} &\frac{\partial T}{\partial x} = 0 \\ &at \quad x = x_F \quad and \\ &at \quad 0 < y < y_F \end{aligned} \tag{8}$$

The equation for absorbed laser beam intensity for TEM_{00} lower order mode, assuming that the laser beam is incident normally, is given as

$$F = aF_o(\hat{n}.\hat{j})e^{\frac{-2((x-ut)^2)}{R^2}}\frac{R_o^2}{R^2} \tag{9}$$

where $\hat{j}$ is a unit vector in the y direction. Laser intensity at the focal plane, F_o is given by:

$$F_o = \frac{2P}{\pi R_o^2} \tag{10}$$

where P is the beam power.

It is assumed that laser beam intensity is uniform at the small solid angle and the particular wavelength involved. For surface absorption, absorptivity of the workpiece is obtained from the reflectivity of the material.

The radius R is a function of the expanding laser beam:

$$R = R(y) = R_o[1 + (\frac{D+y}{\frac{\pi R_o^2}{\lambda_L}})^2]^{\frac{1}{2}} \tag{11}$$

where λ_L is the primary wavelength of the laser beam, D is the distance from the laser focal plane to the material surface, and y is the distance from the surface to the point of depth in the y-direction.

R_o is the laser beam radius at the focal plane which is defined by:

$$2R_o = 0.63\frac{\lambda_L}{N_A} \tag{12}$$

where N_A is the numerical aperture of the laser system, defined by:

$$N_A = 0.5\frac{D_l}{F_l} \tag{13}$$

where D_l is the diameter of the lens and F_l is the focal length of the optical system.

The problem is assumed to be geometrically and thermally symmetric along the y direction. Convective and radiative heat losses on the lateral, upper and bottom surfaces are neglected. The 2-D model is solved by means of FEMLAB version 2.3 code.

IV. FINITE ELEMENT FORMULATION

This is the global formulation of the differential equations representing the appropriate governing equation. Sufficiently continuous trial and weighting functions are required. Using the standard Galerkin approach, the energy balance equation is expressed in variational form. The Galerkin method has the advantage of having the same shape function for both variables and elements. FEMLAB uses the Galerkin method in which the shape functions are the same as the weighting functions.

The finite element formulation begins with the governing differential equation. In general,

$$\rho\dot{U} = -\frac{\partial}{\partial\dot{x}} \bullet \tilde{q} + r \tag{14}$$

Multiplying the above energy equation by an arbitrary variational temperature field, δT and integrating over the full domain(volume) of the body, a variational form of the energy balance equation is obtained.

$$\int_\Omega \rho\dot{U}\delta T d\Omega = -\int_\Omega (\frac{\partial}{\partial\tilde{x}} \bullet \tilde{q})\delta T d\Omega + \int_\Omega r\delta T d\Omega \tag{15}$$

Applying the chain rule to the first term on the right hand side of the above equation gives

$$\int_\Omega \rho\tilde{U}\delta T d\Omega = -\int_\Omega [\frac{\partial}{\partial\tilde{x}}\bullet(\tilde{q}\delta T) + \tilde{q}\bullet\frac{\partial}{\partial\tilde{x}}(\delta T)]d\Omega + \int_\Omega r\delta T d\Omega \tag{16}$$

The divergence theorem is then used to transform the volume integral to a surface integral. Applying the divergence theorem and substituting Fourier's heat conduction law gives:

$$\int_\Omega \rho\tilde{U}\delta T d\Omega + \int_\Omega \frac{\partial\delta T}{\partial\tilde{x}}\bullet k\bullet\frac{\partial T}{\partial\tilde{x}}\delta\Omega = \int_\Gamma q(\delta T)d\Gamma + \int_\Omega r\delta T d\Omega \tag{17}$$

where k is the thermal conductivity matrix.

The domain is now discretized geometrically using finite elements. Assuming the temperature T and temperature gradient $\frac{\partial T}{\partial\tilde{x}}$ within a finite element is interpolated from the nodal temperatures $\bar{T}^N$, it follows that

$$T = N^N\bar{T}^N \quad and \quad \frac{\partial T}{\partial\hat{x}} = \frac{\partial N^M}{\partial\hat{x}}\bar{T}^M \tag{18}$$

where N^M and N^N are the interpolation functions or shape functions and M and N are the number of nodes. Shape functions can be linear or polynomial.

The standard Galerkin approach states that the variational temperature, δT is interpolated with the same functions as temperature. Variational temperature and the temperature gradient is written as:

$$\delta T = N^N\delta\bar{T}^N \quad and \quad \frac{\partial\delta T}{\partial\tilde{x}} = \frac{\partial N^M}{\partial\tilde{x}}\bar{T}^M \tag{19}$$

Substituting these interpolation functions in the heat balance equation gives the following approximation:

$$\begin{aligned}\delta T^N\{&\int_\Omega N^N\rho U d\Omega + \int_\Omega \frac{\partial N^N}{\partial\tilde{x}}\bullet k\bullet\frac{\partial N^M}{\partial\tilde{x}}d\Omega\bar{T}^M \\ &-\int_\Gamma qN^N d\Gamma - \int_\Omega rN^N d\Omega\} = 0\end{aligned} \tag{20}$$

The variational quantities are arbitrary. Equating the term inside the brackets to zero gives

$$\begin{aligned}&\int_\Omega N^N\rho\tilde{U}d\Omega + \int_\Omega \frac{\partial N^N}{\partial\tilde{x}}\bullet k\bullet\frac{\partial N^M}{\partial\tilde{x}}d\Omega\bar{T}^M \\ &= \int_\Gamma qN^N d\Gamma + \int_\Omega rN^N d\Omega = 0\end{aligned} \tag{21}$$

Replacing the change in internal energy with the temperature rate gives

$$\begin{aligned}&\int_\Omega N^N\rho C_p N^M\frac{\partial T^M}{\partial t}d\Omega + \int_\Omega \frac{\partial N^N}{\partial\tilde{x}}\bullet k\bullet\frac{\partial N^M}{\partial\tilde{x}}d\Omega\bar{T}^M \\ &= \int_\Gamma qN^N d\Gamma + \int_\Omega rN^N d\Omega = 0\end{aligned} \tag{22}$$

Equation 23 is the matrix form of the above solution which is easier for computation. Assuming $\{T^e\}$ is the nodal temperature vector, $[C^e]$, the element capacitance matrix, $[K^e]$, elemental conductivity matrix and $\{Q^e\}$, is the elemental load vector, the elemental matrix relation is given as follows:

$$[K^e]\{T^e\} + [C^e]\dot{T}^e = \{Q^e\} \tag{23}$$

where,

$[C^e] = \int_\Omega N^N \rho C_p N^M d\Omega$ is the elemental heat capacity matrix

$[K^e] = \int_\Omega \frac{\partial N^N}{\partial \tilde{x}} \bullet k \bullet \frac{N^M}{\partial \tilde{x}} d\Omega$ is the elemental conductivity matrix

$\{Q^e\} = \int_\Gamma q N^N d\Gamma + \int_\Omega r N^N d\Omega$ is the elemental external flux vector

Using inter-element continuity equations and correspondence between the local and the global nodes, we obtain the global formulation as

$$[A]\{T\} + M\dot{T} = \{B\} \tag{24}$$

where M is the global capacity matrix obtained from the summation of the element capacity matrices. The global conductivity matrix, A and the global load vector, B are obtained from assembling the elemental conductivity and the load vector respectively. The temperature vector is T. The global set of equations is to be solved with specific boundary conditions for the temperature distribution.

V. RESULTS AND DISCUSSION

The finite element model is used to study the process of material removal from a solid surface subjected to a Gaussian laser beam. The displacement of the source generates a phenomenon of trail in the polymer. Figure 3 shows the evolution of temperature according to the coordinate x and at various depths of the polymer. There is low heating in front of the enlightened spot due to diffusion of heat. Heating then grows quickly by absorption of the laser radiation, after which constant temperature is observed. This is due to some balance between heat lost and thermal energy from the laser. This thermal energy deposited by the laser is evacuated by radiative and convective heat transfer and diffusion in the substrate. It is also observed that temperature decreases according to the penetration depth.

It is also observed that low source velocity could increase heating and thermal gradient in the system and worsen mechanical degradation of the material.

The temperature of the sample increases with time while heat diffuses out in the direction of the temperature gradient. Due to the movement of the source, the temperature gradient field also translates. Maximum temperature is obtained under the source. Figure 4 below gives the temperature profile along the direction of motion for several time steps. It shows the thermal development along the heated surface.

Heat diffuses into the material. The greater the depth of the material, the lower the temperature. Figure 5 shows the bulges formed after machining with the laser moving at a velocity of 0.2 m/s. Figure 6 shows a clean cut without bulges at the top

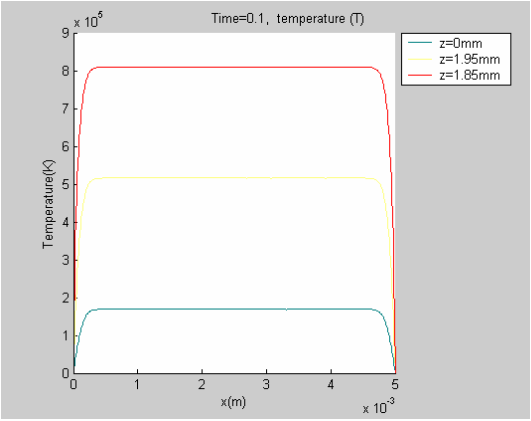

Fig. 3. Temperature distribution x versus z with velocity 0.6m/s.

.

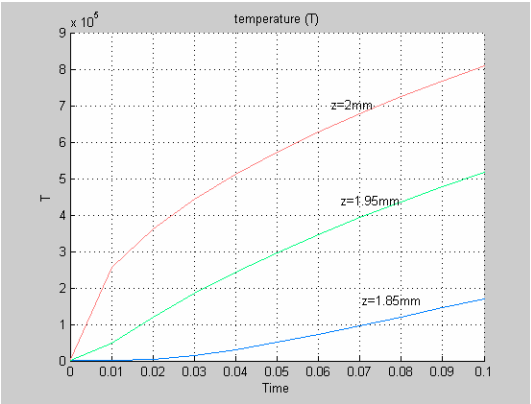

Fig. 4. Temperature distribution with time for velocity 0.6m/s.

.

of the material with the laser moving at a velocity of 0.6m/s. This shows that increase in velocity causes a decrease in the formation of bulges.

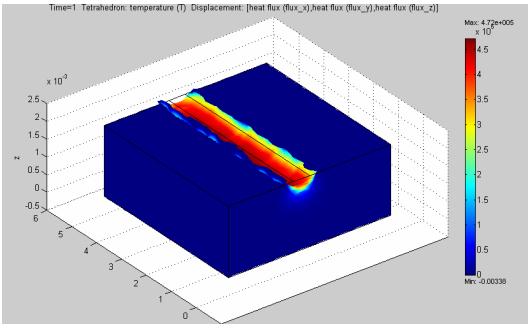

Fig. 5. FEMLAB simulation of laser cutting of PMMA with bulges.

.

Figure 7 shows the relationship between groove depth and scanning velocity of the laser with power of P=30W. Although higher velocity gives a smoother cut, it also cuts a shorter depth, therefore more passes of the laser have to be done to achieve a deep cut.

Figure 8 shows the comparison between experimental values and simulation using FEMLAB. The finite element results are

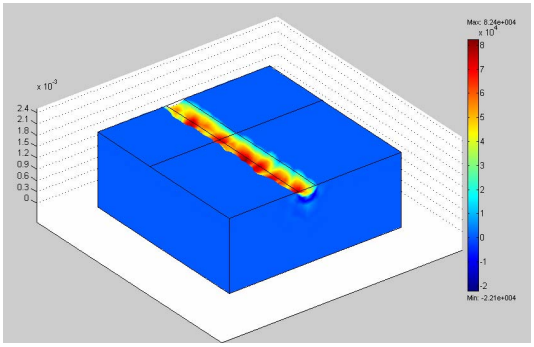

Fig. 6. FEMLAB simulation of laser cutting of PMMA for velocity 0.6m/s.

.

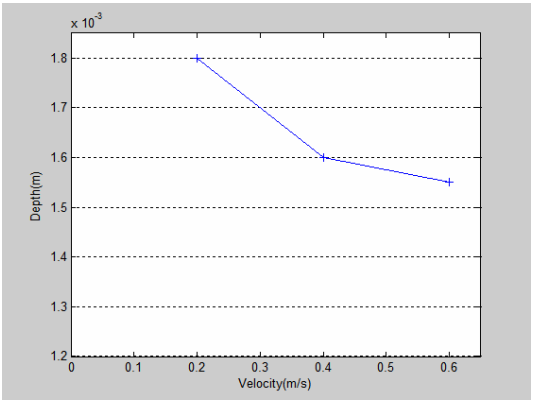

Fig. 7. Relationship between velocity and depth of cut(P=30W).

.

less than the experimental results. This can be attributed to factors neglected by the model such as energy loss due to the erosion front, and that lost due to the resolidified material. The simulation results, however, show good agreement with the experimental results.

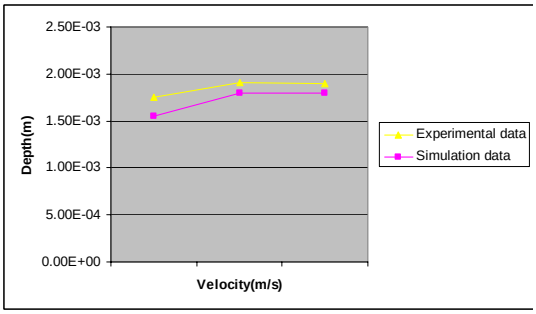

Fig. 8. Contrast between FEM results and experimental data.

.

VI. Conclusion

A model of laser cutting of polymers has been created. FEMLAB 2.3 version was used to construct the model. It is shown that the velocity of the laser affects the formation of the bulge. It is also shown that using low power and higher velocity is more effective in reducing the bulge size. It is realized that FEMLAB is an easy to use computer-based environment that facilitates model development.

Acknowledgment

The authors thank the Jomo Kenyatta University of Agriculture and Technology for availing the funds for this research and the staff members of Mechatronic and Mechanical Engineering Departments for always being ready to assist.

References

[1] C. K. Chung, Y. C. Lin, G. R. Huang , "Bulge formation and improvement of the polymer in carbondioxide laser micromachining," *Journal of Micromechanics and Microengineering*, vol. 15, pp. 1878–1884, 2005.

[2] D. Snakenborg, H. Klank, J. D. Kutter, "Microstructure fabrication with carbondioxide laser," *Journal of Micromechanics and Microengineering*, vol. 14, pp. 182–189, 2004.

[3] Huang Y., Liu S., Yang W. Yu C., "Surface roughness analysis and improvement of pmma-based microfluidic chip chambers by $co_2 laser cutting,'' Applied Surface Science, vol.\ 256, pp.\ 1675 - -1678, 2010$.

[4] D. Rosenthal, "The theory of moving sources of heat and its applications to metal treatments," *Transactions of the ASME*, vol. 1, pp. 849–866, 1946.

[5] M.J. Kim, "3d finite element analysis of evaporative laser cutting," *Applied Mathematical Modelling*, vol. 29, pp. 938–954, 2005.